Eur. Phys. J. D **42**, 61–72 (2007)
DOI: 10.1140/epjd/e2007-00011-3

THE EUROPEAN PHYSICAL JOURNAL D

Local modes of silane within the framework of stretching vibrational polyads

H. Crogman[1], V. Boudon[1], and D.A. Sadovskií[2,a]

[1] Institut Carnot de Bourgogne, UMR 5209 CNRS-Université de Bourgogne, 9 avenue Alain Savary, B.P. 47870, 21078 Dijon, France
[2] Université du Littoral, Département de physique, 59140 Dunkerque, France

Received 9 October 2006 / Received in final form 12 December 2006
Published online 19 January 2007 –

Abstract. We define stretching relative equilibria (RE) of silane and other similar tetrahedral molecules in terms of the dynamical polyad symmetry which assumes the resonance condition 1:1 between the two stretching vibrational modes ν_1 and ν_3 of the molecule. Exploiting symmetry and topology arguments and reducing the dimension of the classical mechanical system, we find these RE. One of them, with local symmetry C_{3v} and minimal energy within a polyad, corresponds to the local modes. We give the upper energy limit of the local mode localization within a polyad.

PACS. 33.15.Mt Rotation, vibration, and vibration-rotation constants – 33.20.Vq Vibration-rotation analysis

1 Introduction

Molecular physicists and theoretical chemists call as local mode a principal stable periodic molecular vibration which is localized primarily on a particular chemical bond. Local modes were used extensively to describe certain vibrational states of nonlinear triatomic molecules — the best known examples are H_2O and O_3 [1,2], and molecules AB_3 and AB_4 with heavy central atom, such as silane [3–7]. The bibliography on the subject is vast and cannot be reviewed in this short paper.

The concept of local modes is closely related to exact or approximate degeneracy of vibrational frequencies. If we consider several linearly independent normal mode vibrations with the same frequency, then in the limit of small vibrations (also called the linearization limit, because in this limit the vibrational Hamiltonian is harmonic and the corresponding equations of motion are linear), local modes reduce to specific linear combinations of degenerated normal modes. Such local modes correspond to specific periodic trajectories, and usually they are called local when the trajectory is stable. In this case, certain excited quantum states are described more physically in terms of local modes because they localize near these modes (and hence near a particular chemical bond). The wavefunction nodes of such states are arranged in a regular pattern with respect to the configuration space image of the mode, and the wavefunctions can be represented as combinations of a few basis wavefunctions describing oscillations along and about the mode. The corresponding part of the classical phase space can be represented as foliated by a continuous family of Liouville tori which converge to the local mode trajectory so that one of their principal cycles becomes this trajectory while other cycles contract to a point. The former cycle corresponds to the motion 'along' the mode, while the other cycles describe oscillations about it.

When using local modes, we should, of course, specify what part of the vibrational energy spectrum can be described more physically in such representation. In other words, we should determine what part of the vibrational states with roughly the same excitation is made up by states localized near these modes. A clear answer to this question has been given for triatomic molecules with two resonant degrees of freedom [2,8–10]. Analysis becomes, obviously, more difficult with growing number of degrees of freedom. In this work, we give the answer for tetrahedral molecules AB_4 with *four* stretching degrees of freedom in resonance and formulate the principles of the analysis of even larger systems, such as bending–stretching polyads of methane which involve *nine* degrees of freedom.

1.1 Nonlinear normal modes

A linearized oscillator system with k degrees of freedom has k normal modes. Recall that when frequencies $\omega_1{:}\cdots{:}\omega_k$ equal nonzero integers $m_1{:}\cdots{:}m_k$ times a common factor ω, we say that modes $1,\ldots,k$ are in resonance $m_1{:}\cdots{:}m_k$. In the absence of such resonance (see Fig. 1,

[a] e-mail: sadovski@univ-littoral.fr

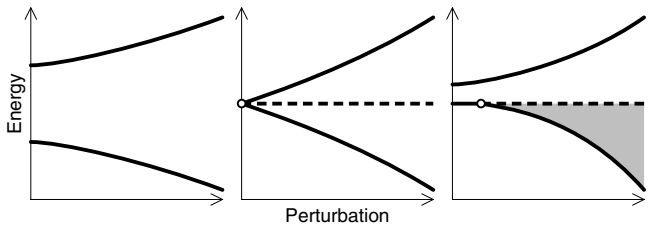

Fig. 1. Energy of nonlinear normal modes of a two-mode system without resonance (left), and in the case of exact (center) and approximate (right) resonances. Families of stable and unstable modes are shown by solid and dashed lines respectively; open circles mark bifurcations; grey shaded area represents local mode states.

left), the k modes *continue* as k families of principal periodic orbits when a typical perturbation is turned on [11]. These orbits are called *nonlinear normal modes*. In the presence of an exact resonance (Fig. 1, center), the situation depends greatly on the particular resonance, symmetries of the system, and the nature of the perturbation [12–14]. Using normal modes to classify all possible dynamical regimes makes rarely sense in this case. In particular, the number of nonlinear modes can be larger than k. Thus, for example, perturbing the double degenerate mode ($k = 2$) of the molecular ion H_3^+, a molecular analog of the Hénon-Heiles system, produces 8 nonlinear normal modes of three different kinds [15] The modes with minimal and maximal energy are stable, while the mode with intermediate energy is unstable; the energy of the unstable mode separates the two types of states localized near different stable modes. A triply degenerate ($k = 3$) vibration F_2 of a tetrahedral molecule AB_4 forms 27 nonlinear normal modes while all 9 vibrational degrees of freedom of AB_4 form 63 such modes [12,13,16].

It follows that we can simplify the analysis by restricting the system only to the modes that are in resonance. However, unless forced by the symmetry of the vibrations involved, molecular resonances are typically not exact. In the case of an approximate resonance (Fig. 1, right), both dynamical regimes are present: for sufficiently small perturbations, resonances can be neglected, while at larger perturbations they become important. Transition between these regimes is marked by one or several bifurcations of nonlinear normal modes.

To have a simple and a well-known example, recall ozone [2]. All three modes of this molecule are nondegenerate and its two stretching modes, symmetric ν_1 and antisymmetric ν_3, are in a close 1:1 resonance. As the system of these two modes enters the resonance regime, the antisymmetric nonlinear normal mode, which is originally stable, bifurcates, loses stability, and sends out two new nonlinear modes which turn out to be the local modes. The bifurcation is of the pitchfork type with broken symmetry of order 2; the new modes are stable, have minimal energy, and are symmetry–equivalent. Quantum states localized near these modes, or 'local mode states', form doublets and ascend to the threshold given by the energy of the unstable asymmetric mode (see shaded area and dashed line Fig. 1, right). Above this energy, we have states which can be considered as excitations of the stable symmetric nonlinear normal mode. Finally, it should be noticed, that the 'size' of the nonresonant region in Figure 1, right, is proportional to the detuning of the resonance. Thus in many systems, including ozone and water, the resonance is so strong that the transition occurs at energies below the energy of the ground state.

In this work we show that the situation in silane is very similar in principle. The frequency ratio of the totally symmetric 'breathing' A_1-type mode ν_1 and the triply degenerate F_2-type mode ν_3 is so close to 1:1 that we can neglect the initial nonresonant regime of 'uncoupled modes'. In other words, the four local modes of silane split off very early. Similarly to ozone, they have minimal energy. Of course we should bear in mind the increased number of degrees of freedom. We now deal with a four-dimensional oscillator in 1:(1:1:1) resonance, where the three ν_3 components are in exact resonance. As a consequence, the ν_3 subsystem itself has several nonlinear normal modes (see [16–19] and compare to Fig. 1, center) of different stability and local symmetry. Furthermore, by the caprice of notation, it is the ν_1 mode of silane which loses stability and serves as upper energy limit for the local mode states, while certain stable nonlinear normal modes associated with ν_3 continue at higher energies.

1.2 Polyads and relative equilibria

Resonances of vibrational modes are at the origin of polyads, or groups of quantum states with the same *polyad quantum number* $N = m_1 n_1 + \ldots m_k n_k$, where $n_1, \ldots, n_k$ are numbers of quanta in each mode. For the 1:1 resonance of ν_1 and ν_3 of silane, this number equals $n_1 + n_3$, where n_3 gives the total number of quanta in the triply degenerate ν_3 mode. Existence of polyads and of good quantum number N corresponds to the existence of a well conserved classical quantity $\mathcal{N}$, i.e., an approximate integral of motion, which we call *polyad integral* and which can be obtained from N by replacing n_i for their classical counterparts $\frac{1}{2}(p_i^2 + q_i^2)$. Thus in the case of silane,

$$\mathcal{N} = \tfrac{1}{2}(p_0^2 + q_0^2) + \tfrac{1}{2}\sum_{i=1}^{3}(p_i^2 + q_i^2),$$

where we use plain indices 0 and $(1, 2, 3)$ for the A_1-mode ν_1 and for the three components of the F_2-mode ν_3, respectively. Notice also that the value n of $\mathcal{N}$ and the quantum polyad number N are related by the quantization rule; in our case (i.e., for an isotropic 4-oscillator), n should be quantized as $N + 2$.

The polyad approximation is very useful for analyzing relatively small vibrations about stable equilibrium configurations of rigid polyatomic molecules. The Hamiltonian flow of $\mathcal{N}$ defines a *dynamical* $\mathbb{S}^1$ *symmetry* which can be reduced. In the case of approximate resonances, such reduction is preceded by normalization of the initial Hamiltonian H with respect to the flow of $\mathcal{N}$. The resulting

normalized Hamiltonian $\mathcal{H}$, or the *normal form*, Poisson commutes with $\mathcal{N}$. Reduced Hamiltonian $\mathcal{H}_n$ is obtained by replacing the conserved quantity $\mathcal{N}$ for its value n. $\mathcal{H}_n$ and its quantum analog $\hat{\mathcal{H}}_n$ are often called model or polyad Hamiltonians. The quantum Hamiltonian $\hat{\mathcal{H}}_n$ describes internal level structure of polyads and is based on a certain assumption of the resonance, i.e., a model. If the molecule has modes other than the ones included in the model, these modes are averaged out from H during normalization and are represented effectively in $\mathcal{H}_n$ by additional parameters. In such case $\mathcal{H}_n$ and $\hat{\mathcal{H}}_n$ are also called effective. Furthermore, when spectroscopists adjust coefficients in front of the terms in $\hat{\mathcal{H}}_n$ to reproduce their experiments, $\hat{\mathcal{H}}_n$ is called phenomenological.

Nonlinear normal modes and local modes as their particular case, have a direct polyad representation. Reduced Hamiltonians $\mathcal{H}_n$ are defined as functions on reduced phase spaces P_n of dimension $2k-2$ ($\mathcal{N}$ represents one universal polyad degree of freedom which is reduced). Topology of P_n depends on the type of resonance and in some cases — on n. Nonlinear normal modes correspond to stationary points of $\mathcal{H}_n$ on P_n. When lifted back to the original phase space $\mathbb{R}^{2k}$ they become periodic orbits of the Hamiltonian flow of $\mathcal{N}$, i.e., $\mathbb{S}^1$ orbits of dynamical symmetry. Such orbits are *relative equilibria*[1] (RE) of the system. So within the polyad approximation, nonlinear normal modes are relative equilibria.

It follows that to find nonlinear normal modes within the polyad approximation we should search for stationary points of $\mathcal{H}_n$ on P_n^{2k-2}, a feasibly simpler task compared to searching for periodic orbits in $\mathbb{R}^{2k}$. Furthermore, we can exploit symmetries of the system to find a set of *isolated fixed points* of the symmetry group action on P_n which is necessarily a subset of all stationary points of $\mathcal{H}_n$. This also provides a classification of RE by their local symmetry which is given by the isotropy group or the stabilizer of corresponding fixed points.

Reduced phase space P_n of a k-mode oscillator in $1{:}\cdots{:}1$ resonance has the topology of complex projective space $\mathbb{C}P^{k-1}$, which we will call for brevity a *polyad space*[2]. Again the most studied and widely known is the case of two modes in 1:1 resonance (see [2,15] for references) where P_n has the topology of a smooth 2-sphere $\mathbb{S}^2$ isomorphic to $\mathbb{C}P^1$. Such case benefited greatly from its analogy to the reduced Euler top which was studied in detail in relation to the description of the structure of rotational multiplets of molecules. Three-oscillator systems with reduced phase space $\mathbb{C}P^2$ have also been studied sufficiently fully in [2,22–24] and in particular for tetrahedral molecules [16,17] with triply degenerate modes. However, since the analysis on $\mathbb{C}P^2$ is, necessarily, more involved and applications are less universal, it remained known only to specialists. Polyad dynamics in the presence of resonances involving $k > 3$ degrees of freedom has never been truly investigated. In a few cases (for example methane with $k = 9$, C_2H_2 with $k = 7$, and of course, silane with $k = 4$), polyads corresponding to such resonances were identified and respective effective polyad Hamiltonians were used to reproduce observed vibrational energy levels. However, the energy level structure was never related to the underlying 'skeleton' of nonlinear normal modes. Furthermore, it is now possible to derive classical and quantum polyad approximations for these molecules directly from their vibrational energy surfaces [25]. Though such approximations are quite accurate in reproducing vibrational (and even rotational) energy level structure, they cannot, obviously, compete with fenomenological fits and the natural use for them is predictions of highly excited localised states using the techniques of our present work. So from this point of view, this work is a considerable step forward.

2 Decomposition of large polyad spaces in terms of polyad subspaces

We now come to the principal idea of the present work. Consider a k-oscillator in $1{:}\cdots{:}1$ resonance and the corresponding polyad space[2] $P_n = \mathbb{C}P_n^{k-1}$ where n is the value of the polyad integral $\mathcal{N}$. Coordinates on P_n can be given using complex Hamiltonian coordinates on $\mathbb{C}^k$,

$$z = q - \mathrm{i}p, \quad \bar{z} = q + \mathrm{i}p,$$

where z, q, and p are k-vectors. Notice that $\mathcal{N} = \frac{1}{2} z\bar{z}$. Points on P_n represent $\mathbb{S}^1$ orbits $z \exp \mathrm{i}\phi_n$ with $\phi_n \in [0, 2\pi)$ and $|z| = \sqrt{2n}$.

We want to take full advantage of possible physically meaningful subspaces of P_n. Thus in particular, we can have several vibrational modes which transform according to different irreducible representations of the symmetry group G of the system. Since the action of G cannot mix these modes, it is natural to retain their coordinates. In other cases it may be important to continue distinguishing specific groups of vibrations, for example bending and stretching.

Consider now two subsystems of our system with k' and k'' modes each and respective polyad integrals $\mathcal{N}'$ and $\mathcal{N}''$, such that $k = k' + k''$, $\mathcal{N} = \mathcal{N}' + \mathcal{N}''$ and $n = n' + n''$. Coordinates on the corresponding polyad spaces $P_{n'} = \mathbb{C}P^{k'-1}$ and $P_{n''} = \mathbb{C}P^{k''-1}$ can be given using coordinates $z = (z', z'')$ on $\mathbb{C}^{k'} \otimes \mathbb{C}^{k''}$. In order to use (z', z'') as coordinates on the whole of P_n we should relate the absolute values $|z'|$ and $|z''|$. To this end we use a *mixing coordinate* $\eta \in [0, 1]$ such that

$$|z'| = \sqrt{\eta}\,\sqrt{2n} \quad \text{and} \quad |z''| = \sqrt{1-\eta}\,\sqrt{2n}.$$

Furthermore, we should also allow for different *relative phases* of z' and z'' by introducing phase difference $\phi = \phi_{n'} - \phi_{n''}$. So for some unit vectors ζ' and ζ'' in $\mathbb{C}'$ and $\mathbb{C}''$, all points on P_n can be represented using

$$z = \sqrt{2n}\left(\sqrt{\eta}\,\zeta',\ \sqrt{1-\eta}\,\exp(\mathrm{i}\phi)\,\zeta''\right). \tag{1}$$

[1] For an introduction to relative equilibria and definitions, see Appendix 5C of [20] and Chapter 3.3 of [21].

[2] In some cases, we will use n as an additional subscript to $\mathbb{C}P_n^{k-1}$ to denote a concrete reduced phase space P_n of topology $\mathbb{C}P^{k-1}$ which represents the constant n level set of $\mathcal{N}$.

Table 1. Representatives of isolated fixed points of the $T_d\times\mathcal{T}$ group action on the ν_3 polyad subspace $\mathbb{C}P^2$ and on the rotational sphere $\mathbb{S}^2$, see [16]. For each type of point we give the class of conjugated subgroups of $T_d\times\mathcal{T}$ to which its stabilizer belongs, and indicate in parentheses the number of equivalent points on $\mathbb{C}P^2$ with stabilizer in the same class.

Stabilizer		ζ_1	ζ_2	ζ_3	j_1	j_2	j_3
$D_{2d}\times\mathcal{T}$	(3)	1	0	0	1	0	0
$C_{3v}\times\mathcal{T}$	(4)	$1/\sqrt{3}$	$1/\sqrt{3}$	$1/\sqrt{3}$	$1/\sqrt{3}$	$1/\sqrt{3}$	$1/\sqrt{3}$
$C_{2v}\times\mathcal{T}$	(6)	$1/\sqrt{2}$	$1/\sqrt{2}$	0	$1/\sqrt{2}$	$1/\sqrt{2}$	0
$S_4\wedge\mathcal{T}_2$	(6)	$1/\sqrt{2}$	$\mathrm{i}/\sqrt{2}$	0	0	0	1
$C_3\wedge\mathcal{T}_s$	(8)	$1/\sqrt{3}$	$\mathrm{e}^{2\mathrm{i}\pi/3}/\sqrt{3}$	$\mathrm{e}^{\mathrm{i}\pi/3}/\sqrt{3}$	$1/\sqrt{3}$	$1/\sqrt{3}$	$1/\sqrt{3}$

To understand better what goes on, one could consider representing $\mathbb{S}^1$ orbits $z\exp\mathrm{i}\phi_n$ in the initial phase space $\mathbb{C}^k$ using their projections $z'\exp\mathrm{i}\phi_{n'}$ and $z''\exp\mathrm{i}\phi_{n''}$ in $\mathbb{C}^{k'}$ and $\mathbb{C}^{k''}$, respectively. Notice also that (η,ϕ) is a variation on the theme of polar coordinates, so we should expect usual problems with ϕ at the 'poles' $\eta=0$ and $\eta=1$.

Applying (1) to the case of (ν_1,ν_3) polyads, let primes and double primes in (1) refer to ν_1 and ν_3 respectively. Then $n'=n_1$, the ν_1 polyad subspace P' is just a point and $\zeta'\equiv 1$, while $n''=n_3$, the ν_3 polyad subspace P'' is a $\mathbb{C}P^2$ space and ζ'' is a three component unit vector $(\zeta_1,\zeta_2,\zeta_3)$ in $\mathbb{C}^3$. Notice also that $\eta=1$ refers to pure ν_1 mode — a single point on $\mathbb{C}P^3_n$, while $\eta=0$ refers to pure ν_3 mode, which is represented by a $\mathbb{C}P^2_n$ subspace of $\mathbb{C}P^3_n$.

3 Polyad spaces and relative equilibria of tetrahedral molecules

3.1 Isolated fixed spaces of the symmetry group action

The full symmetry group of our system $T_d\times\mathcal{T}$ is an extension of the spatial group T_d by time reversal $\mathcal{T}$. Action of $T_d\times\mathcal{T}$ on the ν_3 polyad subspace $\mathbb{C}P^2$ is studied in full detail in [16]. This action has five different kinds of isolated fixed points listed in Table 1. Points of the same kind are symmetry-equivalent, and their energy and stability are the same. So for our purpose, it suffices to have one representative point of each kind.

We can now see the advantage of our coordinates (1) on the (ν_1,ν_3) polyad space $\mathbb{C}P^3$. Thus we can find immediately different isolated fixed $\mathbb{S}^2$ subspaces of $\mathbb{C}P^3_n$ by simply reading $\zeta''=(\zeta_1,\zeta_2,\zeta_3)$ from Table 1. For example, for points on one of these $\mathbb{S}^2$ spheres with stabilizer $D_{2d}\times\mathcal{T}$ we obtain

$$z=\sqrt{2n}\big(\eta^{\frac{1}{2}},\ (1-\eta)^{\frac{1}{2}}\,\mathrm{e}^{\mathrm{i}\phi},0,0\big).$$

Some remarks on the group action are due at this stage. First we draw attention to the simple fact that the $\eta=1$ point on $\mathbb{C}P^3$ has the full $T_d\times\mathcal{T}$ as its stabilizer. This isolated fixed point represents pure ν_1. Next we recall that the action of the T_d group on the ν_3 polyad space $\mathbb{C}P^2$ is equivalent to that of the O group because on this space (z_1,z_2,z_3) and $(-z_1,-z_2,-z_3)$ represent the *same* point and we can extend our symmetry group by an additional operation which mimics spatial inversion and acts trivially on $\mathbb{C}P^2$. However, on the full (ν_1,ν_3) polyad space $\mathbb{C}P^3$, where spatial inversion

$$(z_0,z_1,z_2,z_3)\to(z_0,-z_1,-z_2,-z_3)$$

changes the relative phase $\phi\to\phi+\pi$ between ν_1 represented by z_0 and ν_3 represented by (z_1,z_2,z_3), such extension is no longer possible. This means that the T_d group is more fully represented on $\mathbb{C}P^3$. As a consequence, the action of the six reflection planes of T_d is no longer the same as that of the C_2 axes and there is no fixed spaces $\mathbb{S}^2$ with stabilizer $C_{2v}\times\mathcal{T}$ for $1>\eta>0$. Furthermore, it can be also shown that action of stabilizers $S_4\wedge\mathcal{T}_2$ or $C_3\wedge\mathcal{T}_s$ on the respective points lifted to $\mathbb{C}P^3$ using (1) is not trivial: similar to that of inversion, it changes ϕ (by $\frac{\pi}{2}$ or $\frac{\pi}{3}$ respectively).

3.2 Relative equilibria

From our brief analysis of the group action, we conclude that in the case of stabilizers $C_{2v}\times\mathcal{T}$, $S_4\wedge\mathcal{T}_2$ and $C_3\wedge\mathcal{T}_s$, we have isolated fixed ν_3-points with $\eta=0$. We also have a fully symmetric fixed ν_1-point with $\eta=1$. All these points are necessarily stationary points of any (ν_1,ν_3) polyad Hamiltonian $\mathcal{H}$ and therefore they represent relative equilibria (RE).

More interestingly, mixing of the two modes is allowed for stabilizers $D_{2d}\times\mathcal{T}$ and $C_{3v}\times\mathcal{T}$. In these cases, stationary points of $\mathcal{H}_n$ are confined to the respective invariant $\mathbb{S}^2$ subspaces which we call *coupling spheres*. To find RE with these stabilizers, we should study the restriction of $\mathcal{H}_n(z)$ on these spheres. Such restriction $\mathcal{H}^G_n(\eta,\phi)$ or *coupling function* is, of course, readily obtainable from equation (1) and Table 1 for each stabilizer G. Subsequently, RE are found as stationary points of $\mathcal{H}^G_n$ and are characterized additionally by particular values of ϕ and η.

4 Effective (ν_1,ν_3) polyad Hamiltonian and relative equilibria of silane

The effective Hamiltonian which describes the internal dynamics of the (ν_1,ν_3) polyads can be written to degree four in (q,p) as follows

$$\mathcal{H}=H_0+\mathcal{H}^{11}_2+\mathcal{H}^{33}_2+\mathcal{H}^{13}_2,$$

Table 2. Model effective vibrational Hamiltonian for the (ν_1, ν_3) polyads of silane ($^{28}SiH_4$); parameters are taken from [29] with minor corrections from [28]; notation is explained in footnote 3 on page 65, c.c. stands for the complex conjugate of the preceding expression.

cm^{-1} Parameter		Term	Explicit classical expression
2186.87	ω_1	$\mathcal{N}_1$	$\frac{1}{2}z_0\bar{z}_0$
2189.19	ω_3	$\mathcal{N}_3$	$\frac{1}{2}(z_1\bar{z}_1 + z_2\bar{z}_2 + z_3\bar{z}_3)$
−33.3247	x_0	$H_{11:11}$	$\mathcal{N}_1\mathcal{N}_3$
−34.50104	x_1	$H_{11:02}$	$\frac{1}{4}z_0\,(z_1\bar{z}_2\bar{z}_3 + \bar{z}_1 z_2\bar{z}_3 + \bar{z}_1\bar{z}_2 z_3) + \text{c.c.}$
32.9969	x_2	$H_{20:02}$	$-\frac{1}{8}z_0^2\,(\bar{z}_2^2 + \bar{z}_3^2 + \bar{z}_1^2)/\sqrt{3} + \text{c.c.}$
−34.564	t_1	$H_{20:20}$	$\frac{1}{2}\mathcal{N}_1^2$
−34.6643	$t_3^{A_1}$	$H_{02:02}^{A_1A_1}$	$\frac{1}{24}(z_1^2 + z_2^2 + z_3^2)(\bar{z}_2^2 + \bar{z}_3^2 + \bar{z}_1^2)$
1.920	t_3^{E}	$H_{02:02}^{EE}$	$\frac{1}{24}(z_1^2\bar{z}_1^2 + z_2^2\bar{z}_2^2 + z_3^2\bar{z}_3^2 - z_1^2\bar{z}_2^2 - z_1^2\bar{z}_3^2 - z_2^2\bar{z}_3^2) + \text{c.c.}$
−33.3584	$t_3^{F_2}$	$H_{02:02}^{F_2F_2}$	$\frac{1}{4}(z_1\bar{z}_1 z_2\bar{z}_2 + z_2\bar{z}_2 z_3\bar{z}_3 + z_1\bar{z}_1 z_3\bar{z}_3)$

where

$$H_0 = \omega_1\mathcal{N}_1 + \omega_3\mathcal{N}_3 = \omega_1\mathcal{N} + (\omega_3 - \omega_1)\mathcal{N}_3,$$

and the quartic terms are

$$\begin{aligned}
\mathcal{H}_2^{13} &= x_0 H_{11:11} + x_1 H_{11:02} + x_2 H_{20:02},\\
\mathcal{H}_2^{11} &= t_1 H_{20:20},\\
\mathcal{H}_2^{33} &= t_3^{A_1} H_{02:02}^{A_1A_1} + t_3^{E} H_{02:02}^{EE} + t_3^{F_2} H_{02:02}^{F_2F_2}.
\end{aligned}$$

Further details[3] and respective parameters for silane are given in Table 2. Note that quantum counterparts of vibrational coordinates z and $\bar{z}$ are $\sqrt{2}a$ and $\sqrt{2}a^+$ respectively, where (a^+, a) are vibrational creation-annihilation operators.

The harmonic part H_0 consists of two terms: polyad integral $\mathcal{N}(z, \bar{z})$ with value n and detuning term $\mathcal{N}_3(z, \bar{z})$. We can see from Table 2 that in the case of silane, detuning is of the order of 0.1% of the harmonic frequency and, consequently, the two modes are in a very strong 1:1 resonance. To respect the dynamical symmetry of the system all vibrational operators should Poisson commute with $\mathcal{N}$ and as a consequence, they are of equal degrees in z and $\bar{z}$. (In quantum mechanics this is equivalent to having the same degree in a and a^+ in order to preserve the polyad number N.) The high-order terms describe the effects of three kinds: the (ν_1, ν_3) interaction, the ν_1 nonlinearity and the ν_3 nonlinearity. Construction of quartic terms in Table 2 and notation are similar to that used in [26–28] where more details can be found.

[3] Notation $H_{n_1' n_3' : n_1'' n_3''}^{\Gamma'\Gamma''}$ follows the general notation in [26–28]. It means that the particular term deletes n_i'' quanta and then recreates n_i' quanta in mode $i = 1, 3$. Note that $n_1' + n_3' = n_1'' + n_3''$ for the 1:1 polyad Hamiltonian. When necessary, subscripts Γ' and Γ'' give the final irreducible representation of T_d according to which the respective creation and annihilation factors transform; $\Gamma' = \Gamma''$ for purely vibrational terms.

4.1 Relative equilibria of silane

Using the quartic (ν_1, ν_3) Hamiltonian $\mathcal{H}$ with parameters in Table 2 and the RE coordinates in (1) and Table 1 we computed RE energies, i.e., the values of $\mathcal{H}$ for certain fixed points of the $T_d \times \mathcal{T}$ group action on the polyad space $\mathbb{C}P_n^3$. Results are presented in Figure 3 and Table 3.

In particular we can see that the energy of the RE with symmetry $C_{3v} \times \mathcal{T}$ and $\phi = \pi$ is at the minimum polyad energy. This RE continues from the ν_3 mode at $n = 0$ and gradually increases the ν_1 mode content as indicated by the respective value of η in Table 3. Since, as illustrated in Figure 2, most of the motion of the $C_{3v} \times \mathcal{T}$ RE occurs along one of the four Si–H bonds, this is what theoretical chemists call *local mode*.

At the opposite energy end of the polyad spectrum, we find the $D_{2d} \times \mathcal{T}$ RE which also continues from ν_3 but without taking in any ν_1 contribution (η remains 0). The energy of the ν_1 RE marks roughly the middle of the polyad spectrum. Above this energy, we find several RE of ν_3 origin, and the quantum spectrum is very dense and complicated. The structure below the ν_1 energy is much simpler: local modes exist in this energy range. Transition to the strongly resonant regime with local modes happens at very small n and cannot be seen in Figure 3. Mixing of the ν_1 and ν_3 modes takes place only for a particular pair of equivalent $D_{2d} \times \mathcal{T}$ RE with $\phi = 0$ or π and for all $C_{3v} \times \mathcal{T}$ RE. Further details follow below after we compute the stability of the key RE in this polyad structure.

5 Local approximation and stability of relative equilibria

Local approximations near RE are vital for a more detailed comparison to quantum energy level spectra. In the case of the ν_1, ν_3 polyad with given value n of polyad integral $\mathcal{N}$, the reduced phase space $P_n = \mathbb{C}P_n^3$ is of real dimension six, i.e., locally P_n looks like $\mathbb{R}^6 \sim \mathbb{C}^3$. Consequently, a local approximation near a RE γ is given by

Table 3. Relative equilibria of the (ν_1, ν_3) polyads of silane obtained for the Hamiltonian in Table 2. In the case of $C_{3v} \times \mathcal{T}$, numerical values of η and energy are given for $n = 10$; analytic solutions are obtained in all other cases. Energy of the ν_1 RE (stabilizer $T_d \times \mathcal{T}$) is used as base energy $E_0(n)$ to plot all RE energies in Figure 3.

Stabilizer	ϕ	η (mode)	Energy in units of $\omega_1 = 2186.873$ cm^{-1}
$T_d \times \mathcal{T}$		1 (ν_1)	$n + \frac{1}{2} t_1 \omega_1^{-1} n^2 = n - 0.00790264\, n^2$
$D_{2d} \times \mathcal{T}$		0 (ν_3)	$1.001059\, n - 0.00234912\, n^2$
	$0, \pi$	$0.70271 + 0.03866\, n^{-1}$	$1.000315\, n - 0.00911330\, n^2 - 0.20\, 10^{-4}$
$C_{3v} \times \mathcal{T}$	0	0.177957	9.6839656 for $n = 10$
	0	0.928690	9.1900729 for $n = 10$
	π	0.312896	8.4698469 for $n = 10$
$C_{2v} \times \mathcal{T}$		0 (ν_3)	$1.001059\, n - 0.00638215\, n^2$
$S_4 \wedge \mathcal{T}_2$		0 (ν_3)	$1.001059\, n - 0.00359393\, n^2$
$C_3 \wedge \mathcal{T}_s$		0 (ν_3)	$1.001059\, n - 0.00493827\, n^2$

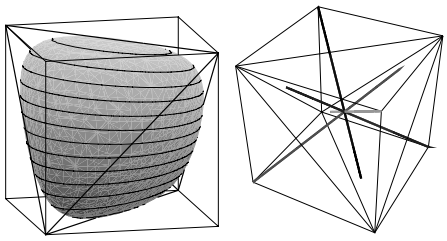

Fig. 2. Representation of the vibrational potential in the ν_3 mode configuration space $\mathbb{R}^3$ with coordinates (q_1, q_2, q_3) (left) and configuration images of four $C_{3v} \times \mathcal{T}$ relative equilibria (bold solid lines, right) for given polyad number $n > 0$ which coincide with A–B bonds of tetrahedral molecule AB_4, see [16] for more details.

a three-mode oscillator Hamiltonian $H_{n,\gamma}(\mathfrak{z})$, normally a Taylor series in $\mathfrak{z}$, defined on the $\mathbb{C}^3$ space or *chart* with coordinates $\mathfrak{z}$ and usual Poisson structure

$$\{\mathfrak{z}_i, \bar{\mathfrak{z}}_i\} = 2\mathrm{i}\, \delta_{ij}, \quad \{\mathfrak{z}_i, \mathfrak{z}_i\} = \{\bar{\mathfrak{z}}_i, \bar{\mathfrak{z}}_i\} = 0, \quad i, j = 1, 2, 3.$$

Local complex Hamiltonian coordinates $\mathfrak{z}$ describe small displacements about the origin $\mathfrak{z} = 0$, which is the image of γ in this chart. Furthermore, since γ is an equilibrium (of the reduced system with polyad Hamiltonian $\mathcal{H}_n$), the lowest degree term $H^0_{n,\gamma}$ in $H_{n,\gamma}(\mathfrak{z})$ is quadratic. Using $H^0_{n,\gamma}$ we can compute linearized equations of motion near and about γ

$$(\dot{\mathfrak{z}}, \dot{\bar{\mathfrak{z}}})^T = A_{n,\gamma}\, (\mathfrak{z}, \bar{\mathfrak{z}})^T.$$

The eigenvalues λ of the 6×6 Hamiltonian matrix $A_{n,\gamma}$ characterize linear stability of γ (as function of dynamical parameter n).

Notice that A is not necessarily diagonal and that a linear symplectic transformation of $(\mathfrak{z}, \bar{\mathfrak{z}})$ might be necessary to obtain a diagonal representation. However, we can simplify this discussion without any loss of generality by assuming that A is already diagonal, i.e., that $(\mathfrak{z}, \bar{\mathfrak{z}})$ is its eigenbasis. Recall also that real and purely imaginary eigenvalues of Hamiltonian matrices come in pairs $\pm\lambda$ while complex eigenvalues form quartets $(\pm\lambda, \pm\bar{\lambda})$ [30].

In the simple situation, when all λ lie on the imaginary axis forming three pairs $(\lambda_i, \bar{\lambda}_i)$, the linearized local Hamiltonian can be written as

$$E_\gamma + H^0_{n,\gamma}(\mathfrak{z}, \bar{\mathfrak{z}}) = E_\gamma + \tfrac{1}{2} \sum_{i=1}^{3} w_i\, \mathfrak{z}_i \bar{\mathfrak{z}}_i, \quad \text{where } w_i = \mathrm{i}\bar{\lambda}_i.$$

If, additionally, the three real frequencies w_i are of the same sign, the respective RE γ is elliptic and stable. For large $\|\mathfrak{z}\|$, nonlinear terms in $H_{n,\gamma}$ become important and at certain energy $h_{n,\gamma}$ of oscillations about γ we may have a barrier, above which the motion is no longer bound. Provided that $h_{n,\gamma}$ is sufficiently large compared to $\hbar \max_i |w_i|$ we should find quantum states localized near RE γ at energies close to the classical energy E_γ. The frequencies w_i define spacings between the energies of these states. Thus the state closest to γ has the energy[4] of $E_\gamma + \frac{1}{2}\hbar \sum w_i$.

It is also important to notice that the ground state of local three-oscillations about γ is itself nondegenerate. However, the total degeneracy of this state is defined by the number of symmetry-equivalent RE γ. Thus in the case of stabilizer $C_{3v} \times \mathcal{T}$ (see Tab. 1) the total degeneracy is *four* — the familiar four local modes [3,4,31,32]. We also say that we have a vibrational 4-*cluster*. In the case of $D_{2d} \times \mathcal{T}$ symmetry we should expect a 3-cluster.

The other simple case occurs when we have pairs $\pm\lambda$ on the real axis. Then the RE γ is hyperbolic and unstable and no quantum localization occurs near it. In all other cases, we should consider nonlinear terms in $H_{n,\gamma}(\mathfrak{z})$ to determine nonlinear stability of γ and describe the energy level structure near E_γ.

Valuable additional information on the eigenvalues λ can be obtained from the symmetry group (stabilizer) G_γ of the relative equilibrium γ [16,17,24]. The local approximation Hamiltonian $H_{n,\gamma}(\mathfrak{z}, \bar{\mathfrak{z}})$ is invariant with respect to elements of G_γ and variables $(\mathfrak{z}, \bar{\mathfrak{z}})$ span a six-dimensional matrix representation $\Gamma_{\mathfrak{z},\bar{\mathfrak{z}}}$ of G_γ. If there is a nontrivial subgroup $SG_\gamma \subseteq G_\gamma$ which acts diagonalwise with respect to the complex structure of $\mathbb{C}^3$ (and which is usually related to the initial spatial symmetry group of the system — in our case T_d) we can also consider a three-dimensional representation $\Gamma_{\mathfrak{z}}$. We can construct $\Gamma_{\mathfrak{z},\bar{\mathfrak{z}}}$ and $\Gamma_{\mathfrak{z}}$ by an explicit analysis of the action of G_γ and SG_γ on $(\mathfrak{z}, \bar{\mathfrak{z}})$ which

[4] Later in this paper we imply the atomic units where $\hbar = 1$.

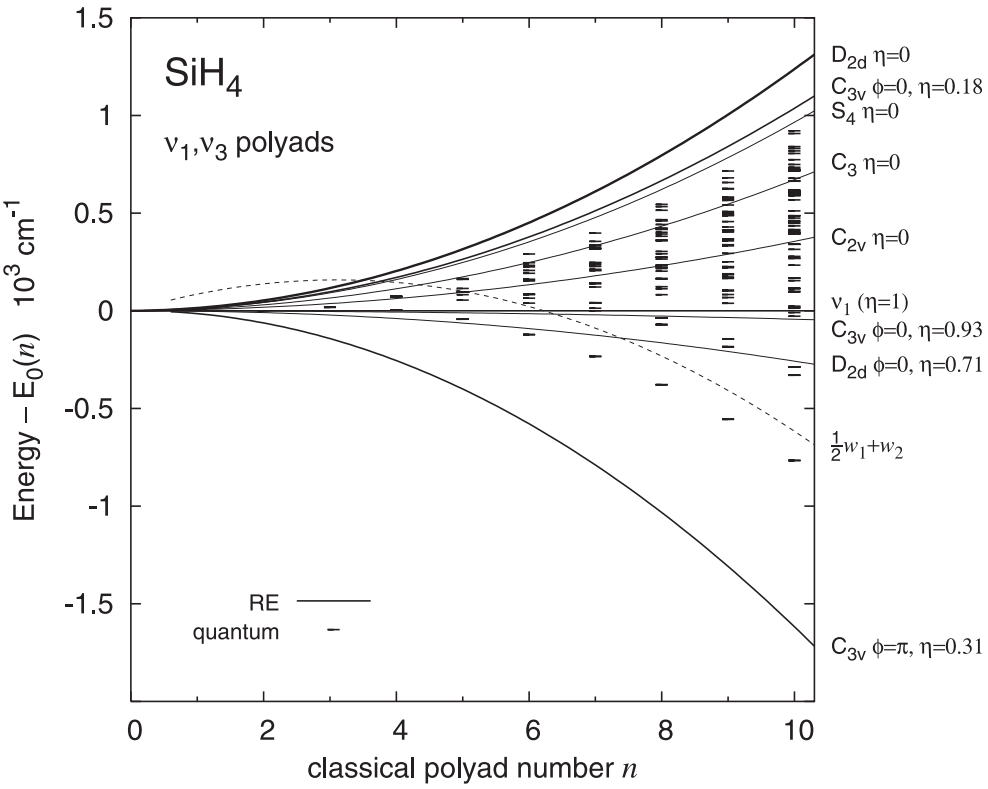

Fig. 3. Energy of relative equilibria (solid lines, see also Tab. 3) and (ν_1, ν_3) vibrational energy levels (short bars) of silane. Energy of the ν_1 RE is used as base energy $E_0(n)$ subtracted from all RE energies; classical action n and polyad quantum number N are related as $n = N + 2$. Dotted line shows harmonic approximation for the energy of the ground state local mode 4-cluster.

derives from that of $T_d \times \mathcal{T}$ on the original vibrational dynamical variables $(z, \bar{z})$ [16,17,24].

Certain general observations can be made even without such detailed analysis. Thus we can see from Table 1 that possible stabilizers G_γ have only irreducible representations of dimension 1 or 2, and $G_\gamma = C_{2v} \times \mathcal{T}$ has only irreducible representations of dimension 1. This restricts possible ways in which $\Gamma_\mathfrak{z}$ and $\Gamma_{\mathfrak{z},\bar{\mathfrak{z}}}$ reduce.

In particular, we will encounter the stable RE with stabilizer $C_{3v} \times \mathcal{T}$, or the local mode RE. In this case, it can be easily shown[5] that $\Gamma_\mathfrak{z}$ reduces into a sum $A \oplus E$ of irreducible representations A and E of respective dimensions 1 and 2, and two of the three local frequencies are necessarily the same (degenerate). This means that the local approximation for $C_{3v} \times \mathcal{T}$ is a stable three-oscillator with one double degenerated mode. The first excited state of this system consists of a single level at frequency w_1 and of a doublet at frequency $w_2 = w_3$. The total degeneracy of such vibrational state is $4 \times (1 + 2) = 12$, or a 4-cluster and a 8-cluster with larger ν_3 presence.

5.1 Computing stability of relative equilibria of the ν_1, ν_3 polyads

We now obtain local approximations near the RE of the ν_1, ν_3 polyads and compute stability of these RE. Our technique is quite general, but for simplicity, we consider only two-block resonances with the concrete application to the ν_1, ν_3 polyads in mind. Let

$$z^0 = (z_0^0, z_1^0, z_2^0, z_3^0) = \sqrt{2n}\,\big(\sqrt{\eta}, \sqrt{1-\eta}\,\mathrm{e}^{\mathrm{i}\phi}\zeta^0\big),$$

with $\zeta^0 = (\zeta_1^0, \zeta_2^0, \zeta_3^0)$ a unit vector in Table 1, be a point on a periodic orbit γ of the flow of the Hamiltonian vector field X_n in $\mathbb{C}^4 \sim \mathbb{R}^8_{q,p}$ which represents a relative equilibrium (RE) of our system. Recall that all points of γ (and z^0 in particular) map to one point on the reduced polyad phase space $\mathbb{C}P^3_n$ and we can use z^0 to represent γ on $\mathbb{C}P^3_n$. Now let $z = z^0 + \mathfrak{z}$ with small $\|\mathfrak{z}\| \ll \sqrt{2n}$ describe points which lie on $\mathbb{C}P^3_n$ near z^0. To describe small oscillations about γ we exploit the definition of the projective space $\mathbb{C}P^3$. In addition we assume that $\eta \neq 0$ and we notice that in this case, according to our choice of z^0

$$\begin{aligned}\operatorname{Re} z_0 &= \operatorname{Re}(z_0^0 + \mathfrak{z}_0) = \sqrt{2n\,\eta} + \operatorname{Re}\mathfrak{z}_0,\\ \operatorname{Im} z_0 &= \operatorname{Im}(z_0^0 + \mathfrak{z}_0) = \operatorname{Im}\mathfrak{z}_0.\end{aligned}$$

In order to define a $\mathbb{C}^3$ chart of $\mathbb{C}P^3$ with origin in z^0, we can impose the following conditions on $z_0 = z_0^0 + \mathfrak{z}_0$

$$\operatorname{Re} z_0 = \sqrt{2n - \sum_{i=1}^{3} z_i \bar{z}_i} = \sqrt{2n - \sum_{i=1}^{3} \|z_i^0 + \mathfrak{z}_i\|^2}, \quad (2a)$$

$$\operatorname{Im} z_0 = 0. \quad (2b)$$

In this local chart, to derive the local expression for energy from the normalized polyad Hamiltonian $\mathcal{H}_n(z_0, z_1, z_2, z_3)$, we replace z_0 by its restricted value

[5] Align coordinate axis q_3 with axis C_3, then components (q_1, q_2) of the F_2 mode ν_3 will span the irreducible representation E of C_{3v}, while A will be spanned by q_3.

Table 4. Linear stability of some (ν_1, ν_3) relative equilibria of silane for $n = 10$ (quantum polyad 8, see Fig. 3), brackets [λ] mark double degenerate eigenvalues, the value of n at which certain RE appear or change stability is indicated as $n_{\rm crit}$.

Stabilizer	ϕ	η (mode)	$n_{\rm crit}$	Eigenvalues in units of ω_1
$D_{2d} \times \mathcal{T}$		0 (ν_3)		0.0612i, [0.0896i]
$C_{3v} \times \mathcal{T}$	0	0.1779	0.071	0.0714i, [0.0448i]
$S_4 \wedge \mathcal{T}_2$		0 (ν_3)	1.301	0.0745, 0.0195i, 0.0183i
$C_3 \wedge \mathcal{T}_s$		0 (ν_3)		0.1108i, 0.0753 ± 0.0354i
$C_{2v} \times \mathcal{T}$		0 (ν_3)		0.1341i, 0.0120 ± 0.1187i
$T_d \times \mathcal{T}$		1 (ν_1)	0.130	0.9255, [0.9497i]
$C_{3v} \times \mathcal{T}$	0	0.9287	~ 0.13	0.1072i, [0.1005]
$D_{2d} \times \mathcal{T}$	$0, \pi$	0.7066	0.130	0.0981, 0.1741i, 0.1407i
$C_{3v} \times \mathcal{T}$	π	0.3129		0.2888i, [0.3134i]

in (2) and represent other coordinates z_i with $i = 1, 2, 3$ as $z_i^0 + \mathfrak{z}_i$. We then Taylor expand $\mathcal{H}_n$ in variables $(\mathfrak{z}_1, \mathfrak{z}_2, \mathfrak{z}_3)$ and obtain local approximation $H_{n,\gamma}(\mathfrak{z})$ near z^0.

In principle, our local chart should work as long as $\eta \neq 0$ and therefore $z_0^0 \neq 0$. The devil is, of course, hidden in the Taylor series expansion of the square root in (2). Indeed, if $z_0^0 = 0$ then $\|(z_1^0, z_2^0, z_3^0)\| = z_1^0\bar{z}_1^0 + z_2^0\bar{z}_2^0 + z_3^0\bar{z}_3^0 = 2n$ and our series simply blows up. In general, this series will be well converging only if $\eta \approx 1$, so that $\|(z_1, z_2, z_3)\|$ remains small and the value under the square root for $(z_1, z_2, z_3) = 0$ is far from 0. If that is not the case, we need to look for an alternative more appropriate chart, where instead of z_0, the role of the eliminated coordinate is played by one of (z_1, z_2, z_3) or by their combination. For example, for $D_{2d} \times \mathcal{T}$ RE (see Tab. 1) with $\eta = 0$ we must eliminate z_1.

Variables (z_1, z_2, z_3) and $(\mathfrak{z}_1, \mathfrak{z}_2, \mathfrak{z}_3)$ inherit the original symplectic structure of $\mathbb{C}^4 \sim \mathbb{R}^8$. They can be, therefore, used immediately to write equations of motion in the chart $\mathbb{C}^3$ and to find the matrix $A_{n,\gamma}$ of their linearization and its eigenvalues λ. At the same time, for each type of RE γ we can find the action of the stabilizer $G_\gamma \subseteq T_d \times \mathcal{T}$ on $(\mathfrak{z}_1, \mathfrak{z}_2, \mathfrak{z}_3)$ from the action of $T_d \times \mathcal{T}$ on (z_1, z_2, z_3) and (z_1^0, z_2^0, z_3^0). Note that $z^0 = (z_0^0, z_1^0, z_2^0, z_3^0)$ is a fixed point of the G_γ action on (z_0, z_1, z_2, z_3) and therefore the origin 0 of the $\mathbb{C}^3(z^0)$ chart is a fixed point of the G_γ on $\mathfrak{z}$. Furthermore, for the local chart under consideration (z_1, z_2, z_3) transform as mode ν_3.

5.2 Stability of relative equilibria of ν_1, ν_3 polyads of silane

Results of our computations for the concrete polyad Hamiltonian of silane in Table 2 are given in Table 4. Three general observations are due here. First, as expected, transition to the strongly resonant vibrational regime occurs in silane very early at $n \approx 0.13$ and way below the value of $n = 2$ for the quantum ground state. This makes a detailed study of bifurcations involved in this transition purely academic as none of these phenomena have any chance to be observed in this particular molecular system. Second, local harmonic frequencies w_1 and w_2 of oscillations about the stable "local mode" RE $C_{3v} \times \mathcal{T}$, $\phi = \pi$ are in a very good agreement with quantum data (see Tab. 5). Third, it is quite interesting to see on our concrete example what other types of stability can exist in such systems. So we comment on them very briefly.

Table 5. Energies in cm^{-1} of quantum states localized near the $C_{3v} \times \mathcal{T}$, $\phi = \pi$ RE of silane, known as local mode, for the $N = 8$ ($n = 10$) polyad. Energies are computed for the polyad Hamiltonian in Table 2 using STDS [26–28] and are given relative to the base energy $E_0 = 20140$ cm^{-1} of the ν_1 RE. Individual states are characterized additionally by their T_d symmetry type; states of type A, E, and F have degeneracy 1, 2, and 3 respectively.

Energy	type	Comments
0		ν_1 RE
−43		RE $C_{3v} \times \mathcal{T}$, $\phi = 0$, $\eta = 0.93$
−286.42	F_1	8-cluster, $n'' = 1$
−286.47	F_2	splitting $\Delta E = 43$, cf. $w_2 - w_1 = 54$
−286.49	E	
−329.46	F_2	4-cluster, $n' = 1$
−329.81	A_1	
−617		classical $\frac{1}{2}w_1 + w_2$
−765.93	$A_1 + F_2$	ground 4-cluster
−1618		local mode RE $C_{3v} \times \mathcal{T}$, $\phi = \pi$

The passage to the resonant regime (cf. Fig. 1, right) can be attributed to $n_{\rm crit} = 0.130$ when the totally symmetric "normal mode" RE ν_1 undergoes a pitchfork bifurcation and becomes hyperbolic in one direction. For $n = 10$ this RE has by far the largest absolute values of the respective eigenvalues: one direction is strongly hyperbolic while oscillations about it in the two other directions are strongly elliptic and have degenerate frequencies. The two RE created in the bifurcation at $n_{\rm crit} = 0.130$ have symmetry $D_{2d} \times \mathcal{T}$ and $\phi = 0, \pi$. These RE are also unstable in one direction.

Comparing this description to Figure 1, note one important difference: in the (ν_1, ν_3) case, the local mode RE ($C_{3v} \times \mathcal{T}$, $\phi = \pi$) does not bifurcate from a normal mode, but continues directly from a pure ν_3 RE at $n = 0$. The eigenvalues λ for this nonlinear mode are second largest by their absolute value. The mode is stable and two oscillations about it have degenerate frequency

$w_2 = \omega_1\lambda_2/\mathrm{i} = 685.3$ cm^{-1} for $n = 10$, while the third local frequency is lower, $w_1 = 631.5$ cm^{-1} for $n = 10$. Using these frequencies, we can estimate the position of the first localized state near this RE at $\frac{1}{2}w_1(n) + w_2(n)$ above the classical RE energy. For $n = 10$ this gives 1001 cm^{-1}, or about a third of the whole (ν_1, ν_3) polyad structure (see Fig. 3).

As we can see from Table 5, this agrees very well with the quantum spectrum which indeed exhibits a large gap between the classical energy minimum and the lowest quantum state, the familiar local mode 4-cluster. Since the above estimate of the gap is obtained in the harmonic approximation, it is slightly higher and the difference gives the idea of the influence of the nonlinear terms in the local approximation. Thus for $n = 10$ the 4-cluster is made of $A_1 + F_2$ states lying 765.93 cm^{-1} below the ν_1 RE energy and 852.1 cm^{-1} above the energy of the classical RE.

Analysis of the lower part of the (ν_1, ν_3) polyad is relatively straightforward. Comparison of the quantum spectrum in Figure 3 and Table 5 to classical RE energies suggests strongly that it is the unstable ν_1 RE (with energy E_0) which serves as an escape route from the local mode potential well. As shown in Figure 3, local harmonic frequencies w_1 and w_2 give qualitatively correct upper estimate of the ground 4-cluster energy. Thus for $n = 10$ (Tab. 5) we obtain $\frac{1}{2}w_1 + w_2 = 1001$ cm^{-1}, which is 150 cm^{-1} above the actual energy of the cluster. Starting from $n = 8$, the depth of the well (1618 cm^{-1} for $n = 10$) is large enough to accommodate the first excited localized state composed of a 4-cluster and a 8-cluster, which lie w_1 and w_2 cm^{-1} above the ground localized state respectively. The splitting between these two components is also well estimated from above by $w_2 - w_1$, see Table 5. The discrepancy of 15–20% can be most certainly explained by considerable anharmonicities of the local mode potential well.

The upper part of the polyad spectrum in Figure 3 looks more complicated. At the maximum energy we find the stable $D_{2d} \times \mathcal{T}$ RE of purely ν_3 origin with single and double local frequencies $w_1 = 134$ and $w_2 = 196$ cm^{-1} respectively for $n = 10$. So we can expect to find the corresponding localized state — a 3-cluster, some 263 cm^{-1} below. Indeed, the quantum spectrum begins about this energy and its topmost state is a 3-cluster whose composition alternates between $E + A$ and F depending on N. The localization pattern for this state can be predicted by comparing to the $D_{2d} \times \mathcal{T}$ nonlinear normal mode in the pure ν_3 case in ([16], Fig. 16 on p. 306). It can be seen that this RE is essentially the F_2 normal mode. So we encounter the general pattern (cf. Fig. 1) with a local mode RE and a normal mode RE at the opposite ends of the polyad energy spectrum.

The situation becomes increasingly more complicated at immediately lower energies due to the presence of another linearly stable RE with symmetry $C_{3v} \times \mathcal{T}$, $\phi = 0$ and small η, i.e., with small ν_1 content. Note that this RE is created in the saddle-node bifurcation on the $C_{3v} \times \mathcal{T}$ invariant coupling space $\mathbb{S}^2$ at $n \approx 0.071$. Immediately below in energy we find the hyperbolic pure ν_3 RE with symmetry $S_4 \wedge \mathcal{T}_2$. It is unclear whether the latter serves as a barrier to either of the two stable RE above it. However, the two complex unstable RE at lower energies $C_3 \wedge \mathcal{T}_s$ and $C_{2v} \times \mathcal{T}$ most certainly put an end to any localization. The presence of complex unstable RE indicates a very interesting polyad dynamics. Due to their existence, this (ν_1, ν_3) system should have monodromy[6] and as a consequence, it cannot be described using a single set of global quantum numbers.

6 Rotational structure

Extension of the present analysis to rotation-vibration follows [16,18] and is relatively straightforward. The full rotation-vibration system has extra degrees of freedom and an additional first integral J, the amplitude of the total angular momentum $\mathbf{J} = (J_1, J_2, J_3)$, with value j. The respective reduced system has the phase space $\mathbb{C}P^3_n \times \mathbb{S}^2_j$, which is a direct product of the vibrational polyad space and the rotational sphere, respectively. Components (J_1, J_2, J_3) restricted by $\|\mathbf{J}\| = j^2$ serve as coordinates on $\mathbb{S}^2_j$.

Terms in the reduced rotation-vibration Hamiltonians for tetrahedral molecules are standardized in [26–28]. Like for any F_2-type mode (see [16,18,19] for details), we have several terms, starting with the linear-in-J Coriolis interaction $T^{1(1,F_1)}_{33}$, which mix different ν_3 components. We note only that due to the large mass of the central atom the $t^{1(1,F_1)}_{33}$ constant of silane is small compared to purely vibrational splittings and that the J^2 terms with constants $t^{2(0,A_1)}_{33}$, $t^{2(2,E)}_{33}$, and $t^{2(2,F_2)}_{33}$ become important at relatively low j. This results in a very dense rotational multiplet without the 'usual' well separated 'Coriolis branches' (cf. [18,19]). Furthermore, many of the RE of interest to us, and in particular the local mode RE, have zero vibrational angular momentum. Such RE do not have energy contributions from $T^{1(1,F_1)}_{33}$ (they belong to the Coriolis Q-branch [16,18]) and therefore, they do not have linear-in-J energy corrections. Rotational corrections to the ν_1 mode energy are similar to the well-known purely rotational terms, whose discussion in terms of rotational RE can be found, for example, in [16,18,38]. We like to mention the principal (ν_1, ν_3) rotational coupling term

$$T^{2(2,F_2)}_{13} = \frac{\sqrt{2}}{3}\big((z_0\bar{z}_1 + \bar{z}_0 z_1)J_2J_3 + (z_0\bar{z}_2 + \bar{z}_0 z_2)J_1J_3 + (z_0\bar{z}_3 + \bar{z}_0 z_3)J_1J_2\big),$$

which is specific to our (ν_1, ν_3) system.

The study of the role of rotation can be done within the same framework. Reduced rotation-vibration Hamiltonian

[6] Hamiltonian monodromy was introduced in [33]; it was largely due to Cushman [34] that molecular physicists became acquainted with this interesting phenomenon. A brief survey of molecular examples can be found in [35]; for more recent developments see [36,37].

Table 6. Rotational contributions to certain coupling functions for the (ν_1, ν_3) polyads; the last row gives the part of rotational contribution which is common to all coupling functions.

Stabilizer	Rotational contribution
$D_{2d} \times \mathcal{T}$	$-\frac{4}{3} t_{33}^{2(2,E)}(1-\eta)\, nj^2 + \frac{16\sqrt{2}}{\sqrt{15}} t^{4(4,A_1)} j^4$
$C_{3v} \times \mathcal{T}$	$-\frac{4\sqrt{2}}{3\sqrt{3}} t_{13}^{2(2,F_2)} \cos\phi \sqrt{\eta(1-\eta)}\, nj^2$
	$-\frac{8}{9} t_{33}^{2(2,F_2)}(1-\eta) nj^2 - \frac{32\sqrt{2}}{3\sqrt{15}} t^{4(4,A_1)} j^4$
common	$t^{2(0,A_1)} j^2 + \left(t_{11}^{2(0,A_1)}\eta + t_{33}^{2(0,A_1)}(1-\eta)\right) nj^2$
	$+ t^{4(0,A_1)} j^4$

$\mathcal{H}_{n,j}(z, \bar{z}, \mathbf{J})$ is a function on $\mathbb{C}P_n^3 \times \mathbb{S}_j^2$ where its equilibrium points represent rotation-vibration RE. To find one such RE γ with stabilizer G_γ, we restrict $\mathcal{H}_{n,j}$ using respective fixed points $(z, \mathbf{J})$ in Table 1 with $\mathbf{J} = j(j_1, j_2, j_3)$. This gives a coupling function $\mathcal{H}_{n,j}^{G_\gamma}(\eta, \phi)$ which, compared to the one we had previously, has the additional parameter j. Examples are given in Table 6. Notice that for all stabilizers in Table 1, rotational coordinates are fixed completely by symmetry, and that $\mathcal{H}_{n,j}^{G_\gamma}(\eta, \phi)$ is, as before, a function on the coupling sphere $\mathbb{S}^2$. At the same time, the number of equivalent RE increases as we should account for two different possible rotation directions inverted by the $\mathcal{T}$ operation.

To describe rotation-vibration RE, we study the stationary points of $\mathcal{H}_{n,j}^{G_\gamma}(\eta, \phi)$ as functions of *two* parameters (n, j). Such analysis is beyond the scope of our present discussion. We point out, however, that $\mathcal{H}_{n,j}^{G}$ with $G = C_{3v} \times \mathcal{T}$ is the only coupling function that gets a contribution from the rotation-vibration coupling term $T_{13}^{2(2,F_2)}$. This makes analysis of the influence of rotation on the RE with stabilizer $C_{3v} \times \mathcal{T}$ and $0 < \eta < 1$, including the local mode RE, particularly interesting.

7 Conclusions

Our present analysis complements greatly the earlier work on local modes (see for example [3–7] and others) in two important aspects. First, we present local modes within the global polyad framework where a local mode is a particular stable nonlinear normal mode (or, equivalently, RE). This relates local modes most directly to the general approach of describing "rigid" polyatomic molecules in the limit of small (and not-so-small) vibrations [39–41], such as the STDS formalism [26–28] developed for tetrahedral molecules AB_4, as well as to other local mode and polyad studies. Second, we also provide precise limits of the existence of quantum states localized near the local mode RE of silane, and show what part of the total vibrational polyad spectrum these states occupy.

Despite the obvious difficulty of extending polyad studies to systems with large number of internal polyad degrees of freedom, we succeeded in finding a number of important RE and relating them to the quantum spectrum. It is clear, however, that for any comprehensive study of the (ν_1, ν_3) system, our work provides just a good starting point. The main remaining problem is the global dynamical analysis on the polyad space $P_n = \mathbb{C}P_n^3$, i.e., the study of dynamical connections between the different RE we found. Thus, for example, it remains to prove, that the ν_1 RE and not the two unstable RE with energies below that of ν_1 is the escape route from the local mode potential well. Such a task is, in a sense, similar to theoretical chemistry studies of a reaction path on a multidimensional potential surface, albeit here we deal with multidimensional Hamiltonian dynamics on a curved multidimensional space.

The other way to formulate the problem, is to notice that we lack additional characteristics of internal polyad dynamics: the number of internal polyad degrees of freedom has risen, but the number of characteristics available globally is the same — energy and the value n of the polyad integral (polyad number N). Indeed, in the absence of any additional Lie symmetries, our reduced system on P_n is not integrable. In general, we can only attempt to introduce local first integrals for local approximations near RE and use appropriate techniques to assign additional local labels to quantum wavefunctions. Connecting between different local approximations brings us back to the above formulated problem of global analysis.

From this point of view, we were somewhat "lucky" that the sequence of local mode clusters between the ν_1 RE and the $C_{3v} \times \mathcal{T}$, $\phi = \pi$ RE was not obscured by any other sequences of quantum levels and could be analyzed easily without any additional first integrals, respective local quantum numbers and techniques of their assignment. The upper part of the (ν_1, ν_3) polyads of silane cannot be analyzed that easily. Looking at the dense and seemingly incomprehensible quantum spectrum above the ν_1 RE energy, one should, however, be cautious about writing off any further analysis in this part in terms of regular dynamics. We can be dealing with several systems of states which overlap in energy but which are localized in different regions of the phase space P_n, and thus described by different local quantum numbers. In this regard, particularly interesting is a local study near each of the two complex unstable RE which may uncover two different subsystems of quantum states with monodromy.

Notice also that our RE analysis itself is quite basic and unfinished. We only found RE which are defined (almost entirely) by symmetry, while other RE situated on higher dimensional noncritical strata of the group action may exist. Studying bifurcations (many at low n) of the known RE and using global topological arguments of the Morse theory may help finding them. Such study is beyond both the purpose and the volume of our present work.

8 Perspectives

Any serious spectroscopic application requires a complete rotation-vibration analysis. In the particular system, the interesting question to answer is whether rotation affects

qualitatively the existence and stability of the $C_{3v} \times \mathcal{T}$ RE, and of the local mode RE in particular. The question whether localization near a RE is of 'rotational' or 'vibrational' origin can be answered by studying j and n contributions to the coupling function. Thus, if new RE appear at large j, we can associate them with rotation.

Another important direction is local rotation-vibration Hamiltonians near stable RE. For the local mode minimum, such a Hamiltonian was used in [3–7,32,42]. As can be expected, it represents a non-rigid symmetric top and inherits the $C_{3v} \times \mathcal{T}$ symmetry of the RE. In general, local Hamiltonians can be readily constructed using the methods we developed here for the stability analysis, and their parameters can be related to those of the full polyad Hamiltonian $\mathcal{H}_{n,j}$. We can subsequently use a local Hamiltonian to analyze the fine structure of rotation-vibration bands which involve only a group of states localized near a particular RE. In some cases, we can make further adjustments of its parameters, which make a small subset of all parameters of $\mathcal{H}_{n,j}$, in order to reproduce these bands more finely.

The interest in transitions to localized states is obvious: in the sea of irregular quantum states, which we are bound to encounter at high excitations, they provide regular and easily recognizable spectra. This brings us to the problem of describing intensities of such transitions. Again, we can do this by expanding the polyad transition moment near the RE of interest using the techniques in this paper. In this way we can ascribe 'transition moments' $\mu_\gamma(n)$ to each RE γ, i.e., to each nonlinear normal mode, and find respective 'oscillator strengths' $f_\gamma(n', n'')$.

Our technique can be used in many systems with multiple resonances. Among them, methane (CH_4), a basic molecule and an important ingredient of terrestrial and planetary atmospheres, can be considered as an ultimate goal. Methane has huge and complex polyads with no visible 'local modes'. At the same time, observations of transitions with large $n' - n''$ show intriguing intense regular structures which may indicate the presence of very stable RE and respective localized states. Analysis of such transitions on the basis of traditional well developed spectroscopic techniques [26–28] runs into obvious difficulties due to enormous numbers of individual excited quantum states. In this situation, uncovering localized states first becomes a necessity and using our approach — the most promising way forward.

We thank Professor B.I. Zhilinskiĭ for many valuable discussions and for critical reading of the manuscript. HC thanks Région Bourgogne for support (postdoctoral fellowship 04 HCP 62).

References

1. J.T. Muckerman, M.S. Child, Chem. Phys. Lett. **153**, 477 (1988)
2. I.N. Kozin, D.A. Sadovskiĭ, B.I. Zhilinskiĭ, Spectrochim. Acta A **61**, 2867 (2005)
3. L. Halonen, M.S. Child, Comp. Phys. Communs. **51**, 173 (1988)
4. M.S. Child, Qing-shi Zhu, Chem. Phys. Lett. **184**, 41 (1991)
5. M. Chevalier, A. De Martino, F. Michelot, J. Mol. Spectrosc. **131**, 382 (1988)
6. C. Leroy, F. Michelot, J. Mol. Spectrosc. **151**, 71 (1992)
7. C. Leroy, F. Michelot, V. Boujut, J. Mol. Spectrosc. **173**, 333 (1995)
8. K. Stefanski, E. Pollak, J. Chem. Phys. **87**, 1079 (1987)
9. L. Xiao, M.E. Kellman, J. Chem. Phys. **90**, 6086 (1989)
10. Z.-M. Lu, M.E. Kellman, J. Chem. Phys. **107**, 1 (1997)
11. A. Weinstein, Invent. Math. **20**, 47 (1973)
12. J. Montaldi, R.M. Roberts, I. Stewart, Phil. Trans. R. Soc. Lond. A **325**, 237 (1988)
13. J. Montaldi, M. Roberts, I. Stewart, Nonlinearity **3**, 695 (1990)
14. J. Montaldi, M. Roberts, I. Stewart, Nonlinearity **3**, 730 (1990)
15. D.A. Sadovskiĭ, N.G. Fulton, J.R. Henderson, J. Tennyson, B.I. Zhilinskiĭ, J. Chem. Phys. **99**, 906 (1993)
16. K. Efstathiou, D.A. Sadovskiĭ, B.I. Zhilinskiĭ, SIAM J. Appl. Dyn. Syst. (SIADS) **3**, 261 (2004)
17. K. Efstathiou, D.A. Sadovskiĭ, Nonlinearity **17**, 415 (2004)
18. Ch. Van Hecke, D.A. Sadovskiĭ, B.I. Zhilinskiĭ, V. Boudon, Eur. Phys. J. D **17**, 13 (2001)
19. G. Dhont, D.A. Sadovskiĭ, B.I. Zhilinskiĭ, V. Boudon, J. Mol. Spectrosc. **201**, 95 (2000)
20. Vl.I. Arnol'd, *Matematicheskie Metody Klassicheskoĭ Mekhaniki* (Nauka, Moscow, 1974), in Russian; *Mathematical Methods of Classical Mechanics*, translated by K. Vogtmann, A. Weinstein, 2nd edn., ser. Graduated Texts in Mathematics **60** (Springer-Verlag, New York, 1989)
21. Vl.I. Arnol'd, V.V. Kozlov, A.I. Neĭshtadt, *Mathematical Aspects of Classical and Celestial Mechanics*, Dynamical Systems III, Encyclopedia of Mathematical Sciences **3** (Springer-Verlag, Berlin, 1988)
22. B.I. Zhilinskiĭ, Chem. Phys. **137**, 1 (1989)
23. D.A. Sadovskiĭ, B.I. Zhilinskiĭ, Phys. Rev. A **48**, 1035 (1993)
24. K. Efstathiou, D.A. Sadovskiĭ, R.H. Cushman, Proc. Roy. Soc. Lond. A **459**, 2997 (2003)
25. X.-G. Wang, E.L. Sibert, J. Chem. Phys. **113**, 5384 (2000)
26. J.-P. Champion, M. Loëte, G. Pierre, in *Spectroscopy of the Earth's Atmosphere and Interstellar Medium*, edited by K.N. Rao, A. Weber (Academic Press, San Diego, 1992)
27. Ch. Wenger, J.-P. Champion, J. Quant. Spectrosc. Radiat. Transfer **59** 471 (1998)
28. *Spherical Top Data System (STDS)*: a computer package for simulation of spherical top spectra, available from url `http://icb.u-bourgogne.fr/OMR/SMA/STDS.html`
29. J.C. Hilico et al., J. Mol. Spectrosc. **168**, 455 (1994)
30. J. Williamson, Amer. J. Math. **58**, 141 (1936); J. Williamson, Amer. J. Math. **59**, 599 (1937)
31. L. Halonen, J. Chem. Phys. **106**, 831 (1997)
32. M. Halonen, L. Halonen, H. Burger, W. Jerzembeck, J. Chem. Phys. **108**, 9285 (1998)
33. J.J. Duistermaat, Comm. Pure Appl. Math. **33**, 687 (1980)
34. R.H. Cushman, L. Bates, *Global aspects of classical integrable systems* (Birkhauser, Basel, 1997)
35. K. Efstathiou, M. Joyeux, D.A. Sadovskiĭ, Phys. Rev. A **69**, 032504 (2004)

36. R.H. Cushman, H.R. Dullin, A. Giacobbe, D.D. Holm, M. Joyeux, P. Lynch, D.A. Sadovskiĭ, B.I. Zhilinskiĭ, Phys. Rev. Lett. **93**, 024302 (2004)
37. B.P. Winnewisser, M. Winnewisser, I.R. Medvedev, M. Behnke, F.C. De Lucia, S.C. Ross, J. Koput, Phys. Rev. Lett. **95**, 243002 (2005)
38. Ch. Van Hecke, D.A. Sadovskiĭ, B.I. Zhilinskiĭ, Eur. Phys. J. D **7**, 199 (1999)
39. E.B. Wilson Jr, J.C. Decius, P.C. Cross, *Molecular Vibrations* (McGraw-Hill, New York, 1955)
40. G. Amat, H.H. Nielsen, G. Tarrago, *Rotation-vibrations of polyatomic molecules* (Dekker, New York, 1971)
41. M.R. Aliev, J.K.G. Watson, *Higher-order effects in the vibration-rotation spectra of semirigid molecules*, in Molecular Spectroscopy: Modern Research, edited by K.N. Rao (Academic Press, New York, 1985), Vol. 3, p. 1.
42. T. Lukka, L. Halonen, J. Chem. Phys. **101**, 8380 (1994)